

Strain relaxation of pseudomorphic $\text{Si}_{1-x}\text{Ge}_x/\text{Si}(100)$ heterostructures after Si^+ ion implantation

B. Holländer, D. Buca, M. Mörschbacher, St. Lenk, and S. Mantl
*Institut für Schichten und Grenzflächen (ISGI) and cni - Center of Nanoelectronic Systems
 for Information Technology, Forschungszentrum Jülich GmbH, D-52425 Jülich, Germany*

H.-J. Herzog and Th. Hackbarth
DaimlerChrysler AG, Research and Technology, D-89081 Ulm, Germany

R. Loo and M. Caymax
IMEC, Kapeldreef 75, B-3001 Leuven, Belgium

P. F. P. Fichtner
*Departamento de Metalurgia, Universidade Federal do Rio Grande do Sul,
 BR-91501-970 Porto Alegre, Brazil*

(Received 1 March 2004; accepted 30 April 2004)

The strain relaxation of pseudomorphic $\text{Si}_{1-x}\text{Ge}_x$ layers ($x=0.21, \dots, 0.33$) was investigated after low-dose Si^+ ion implantation and annealing. The layers were grown by molecular-beam epitaxy or chemical vapor deposition on $\text{Si}(100)$ or silicon-on-insulator. Strain relaxation of up to 75% of the initial strain was observed at temperatures as low as 850 °C after implantation of Si ions with doses below $2 \times 10^{14} \text{ cm}^{-2}$. We suggest that the Si implantation generates primarily dislocation loops in the SiGe layer and in the underlying Si which convert to strain relaxing misfit segments. The obtained results are comparable to strain relaxation achieved after He^+ implantation with doses of $1-2 \times 10^{16} \text{ cm}^{-2}$. © 2004 American Institute of Physics. [DOI: 10.1063/1.1765851]

Strained Si films grown on strain-relaxed SiGe buffer layers will soon be applied for advanced microelectronic devices since strained Si exhibits significantly enhanced carrier mobilities and therefore, yields to transistors with higher transconductance and drive currents.^{1,2} However, a key problem is the fabrication of thin strain relaxed SiGe buffer layers, which serve as virtual substrates for the growth of strained silicon. The standard approach is the growth of several micrometer thick, compositionally graded buffer layers.³ Recently, it was shown that He^+ ion implantation and subsequent thermal annealing can successfully be employed to relax the strain of thin pseudomorphic SiGe layer grown on $\text{Si}(100)$.⁴⁻⁶ The required He^+ implantation doses to achieve substantial strain relaxation during the subsequent annealing are in the range of $5 \times 10^{15} \text{ cm}^{-2}$ to $2 \times 10^{16} \text{ cm}^{-2}$. These relatively high doses lead to long implantation times and limit throughput of wafers in production and form voids in the underlying silicon. Previously it was shown that strain relaxation can also be achieved by H^+ implantation and annealing.⁴ However, this method was only successful for SiGe layers with Ge concentrations below 25 at. %. Enhanced strain relaxation due to the introduction of point defects by Ge^+ ion implantation at 400 °C or the implantation of dopants (B, As) was reported, however, without revealing the resulting microstructure.^{7,8} The use of ion implantation for strain relaxation has several advantages: It is easy to use, is highly reproducible, is area-selective by the use of masks, and is fully compatible with existing Si technology. Therefore, there is interest in the development of an ion implantation method, which allows efficient strain relaxation after annealing at moderate temperatures while maintaining a high

sample quality. It is important to use ions, which require only a low dose and avoid contamination or unintended doping by the implanted ions.

In this work, we have investigated the strain relaxation of pseudomorphic $\text{Si}_{1-x}\text{Ge}_x$ layers induced by low dose Si^+ ion implantation at room temperature and subsequent annealing. We also provide a preliminary explanation for the mechanism of strain relaxation. The layers were grown by chemical vapor deposition (CVD) and solid-source molecular-beam-epitaxy (MBE) on $\text{Si}(100)$ and on silicon-on-insulator (SOI) wafers. The samples were characterized using transmission electron microscopy (TEM) at 400 kV in a JEOL 4000 FX microscope, Rutherford backscattering spectrometry (RBS), and ion channeling with 1.4 MeV He^+ ions at a scattering angle of 170°. The initial strain as well as the amount of strain relaxation was determined by ion channeling angular scans along a (100) plane through the [100] sample at normal and an inclined [110] direction. In a SiGe layer under compressive strain, the angle between the [100] and [110] directions is smaller than 45° and the angular deviation can directly be converted into the amount of tetragonal strain.⁵ We compared these results with high resolution x-ray diffraction data and found consistent agreement within 5%. Details of the technique of strain measurement by ion channeling and a comparison to XRD measurements are given in Ref. 5.

Figure 1 shows random and [100] channeling spectra (solid lines) of a CVD-grown, 180 nm thick $\text{Si}_{0.79}\text{Ge}_{0.21}$ layer on $\text{Si}(100)$. Layer thickness and Ge concentration were determined by RBS and the use of the RUMP simulation code.⁹ The minimum yield of less than 3% indicates a high crystalline quality of the SiGe layer. No increase of the ratio of

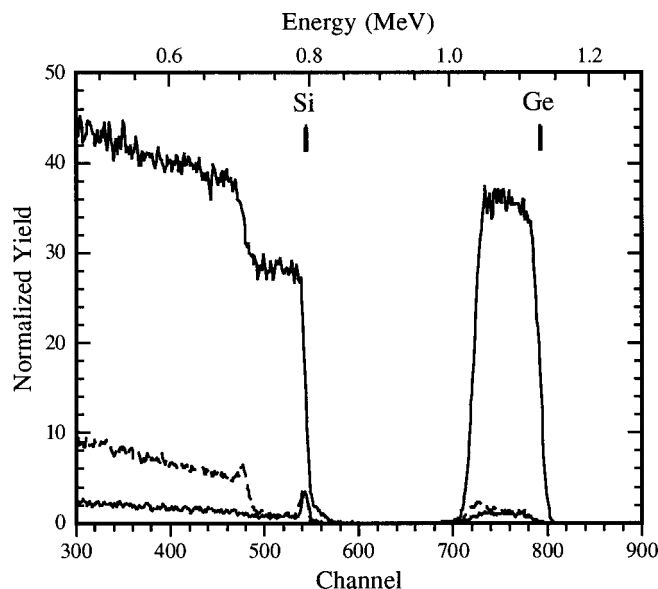


FIG. 1. Random and [100] channeling spectra (solid lines) of a CVD-grown, 180 nm thick $\text{Si}_{0.79}\text{Ge}_{0.21}$ layer on Si(100). The dashed line represents the channeling spectrum after implantation of 195 keV Si^+ ions with a dose of $1.5 \times 10^{14} \text{ cm}^{-2}$ and annealing at 850°C for 600 s.

channeling to random yield is observed at the SiGe/Si interface (channel no. 480). Strain measurements revealed that the sample is fully strained according to its Ge content. The dashed line in Fig. 1 represents the channeling spectrum after implantation of 195 keV Si^+ ions with a dose of $1.5 \times 10^{14} \text{ cm}^{-2}$ and annealing at 850°C for 600 s in Ar atmosphere. At this energy the Si ions are stopped about 100 nm below the SiGe/Si interface. The significant increase of the channeling yield due to dechanneling at the interface is attributed to the formation of a high density of misfit dislocations leading to strain relaxation. The angle of 44.893° between the [100] surface normal and an inclined [110] direction was determined by channeling angular yield scans.⁵ For a fully strained SiGe layer, this angle amounts to 44.590° . This corresponds to a strain relaxation of 74% of the initial strain. At the same time, no increase of dechanneling was observed close to the surface of the SiGe layer indicating that the high crystalline quality of the SiGe layer is maintained after relaxation. A cross section TEM micrograph (Fig. 2) exhibits a strong contrast at the interface due to the misfit dislocation network. No threading dislocations were found by cross-section transmission electron microscopy (XTEM). Additional plan-view (TEM) investigations re-

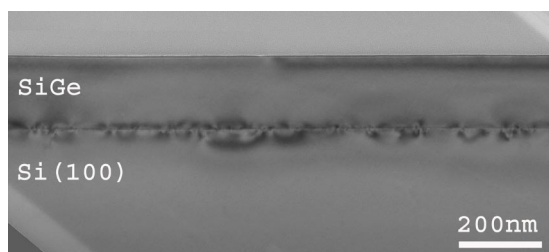


FIG. 2. The cross section TEM micrograph of the implanted and annealed sample shown in Fig. 1 exhibits a strong contrast at the interface due to the misfit dislocation network.

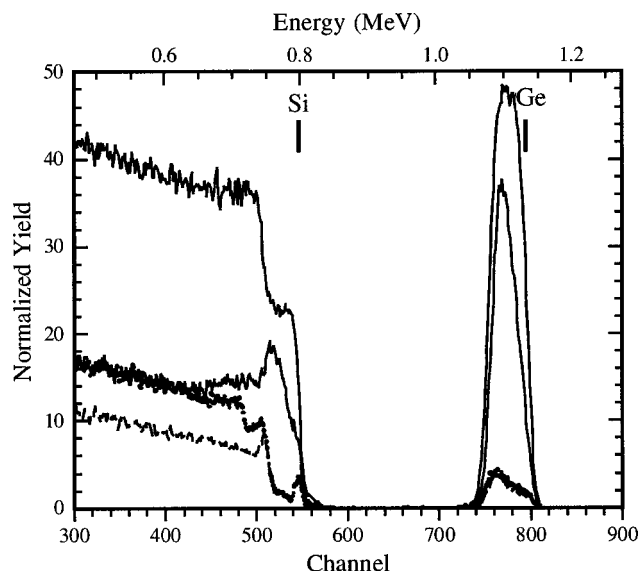


FIG. 3. Comparison of Si and He ion implantation for strain relaxation. Random RBS spectrum of a MBE-grown 100 nm thick $\text{Si}_{0.70}\text{Ge}_{0.30}$ layer on Si(100) together with a [100]-channeling spectrum of the sample after implantation of 150 keV Si^+ ions with a dose of $1 \times 10^{14} \text{ cm}^{-2}$ (solid lines). The dashed line represents the channeling spectrum after annealing at 850°C for 600 s. The channeling spectrum of a reference sample implanted with 18 keV, $2 \times 10^{16} \text{ He}^+/\text{cm}^2$ instead of Si^+ ions is shown for comparison (dotted line).

vealed the lowest threading dislocation density of $3 \times 10^7 \text{ cm}^{-2}$ for a sample annealed at 950°C . Further optimization of implantation and annealing conditions is under investigation. A very small rms surface roughness of 0.45 nm was measured by atomic force microscopy (AFM), which is similar to that of He implanted samples. In comparison, the rms roughness before implantation is typically 0.3 nm. The implantation dose is a critical issue. For doses of $1 \times 10^{14} \text{ cm}^{-2}$ and $2 \times 10^{14} \text{ cm}^{-2}$ we obtained relaxation degrees of 17% and 67%, respectively; in the latter case the sample was of poor crystalline quality, as judged from axial channeling measurements.

SiGe layers with higher Ge content were grown by MBE on Si(100) and implanted with Si^+ ions and annealed. Figure 3 shows a random RBS spectrum of a 100 nm thick $\text{Si}_{0.70}\text{Ge}_{0.30}$ layer on Si(100) together with a [100]-channeling spectrum of the sample after implantation of 150 keV Si^+ ions with a dose of $1 \times 10^{14} \text{ cm}^{-2}$ (solid lines). Pronounced dechanneling within the SiGe layer is an indication of the implantation induced lattice defects, which extend to a depth of about 100 nm below the SiGe/Si interface. A lower channeling-to-random ratio in Si compared to SiGe could be attributed to a lower sensitivity to ion beam damage in Si compared to SiGe. After annealing at 850°C for 600 s the heterostructure recovers from the ion damage indicated by a low backscattering yield of the channeling spectrum (dashed line). The strong increase of the channeling spectrum at the interface (channel 520) is attributed to the formation of misfit dislocations leading to strain relaxation. Ion channeling angular yield scans revealed a strain relaxation of 78% of the initial strain. For comparison, the channeling spectrum of a reference sample implanted with 18 keV, $2 \times 10^{16} \text{ He}^+/\text{cm}^2$ instead of Si^+ ions is shown in

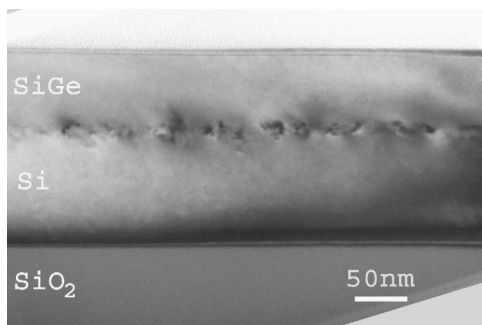


FIG. 4. XTEM micrograph of 88 nm $\text{Si}_{0.67}\text{Ge}_{0.33}$ grown on a SOI wafer after implantation and annealing. Misfit dislocations at the SiGe/Si interface are clearly visible.

Fig. 3 (dotted line) after the same anneal. The amount of dechanneling within the SiGe layer as well as a strain relaxation of 78% is comparable to the case of Si implantation. However, the He implanted sample shows an additional dechanneling peak (channel 480) due to the cavities formed at about 100 nm below the interface, which remain after the anneal.¹⁰

Furthermore, we applied Si^+ ion implantation on an 88 nm thick $\text{Si}_{0.67}\text{Ge}_{0.33}$ layer grown by MBE on a 100 nm SOI substrate. The sample was implanted with 150 keV Si^+ ions with a dose of $1 \times 10^{14} \text{ cm}^{-2}$ and annealed at 850 °C for 600 s. Channeling investigations indicated, similar to Fig. 3, more damage in the SiGe layer than in the underlying 100 nm thick Si layer after implantation (not shown). The crystal lattice recovered after annealing nearly to the as-grown quality as proved by channeling (not shown). The XTEM micrograph of Fig. 4 shows a clear contrast due to the strain relaxing misfit dislocations at the Si/SiGe interface but no threading dislocations in the strain relaxed SiGe layer. Channeling angular yield scans revealed a relaxation of 75% of the initial strain, which is comparable to the strain relaxation of 77% obtained after 13 keV He^+ implantation with a dose of $1.5 \times 10^{16} \text{ cm}^{-2}$ and subsequent annealing.

Previously, we proposed a model for the strain relaxation mechanism for the case of H or He implantation into pseudomorphic SiGe layers.¹¹ According to this model, H or He high pressure bubbles eject dislocation loops which glide to the Si/SiGe interface and convert into strain relaxing misfit dislocations. These misfit segments are unavoidably accompanied with the threading dislocations in the SiGe, which, however, are able to annihilate efficiently during subsequent annealing. Interestingly, Si implantation and annealing produces also a high density of dislocation loops below the SiGe interface under the used conditions, although their formation mechanism is different. In the case of self-ion implantation in silicon the residual damage is dominated by interstitial-type defects as a direct consequence of an extra implanted ion. The so-called “+1” model suggests that upon annealing, vacancies and interstitials recombine leaving excess interstitials equal in number to the dose of the implanted ions.^{12,13}

TEM investigations after 100 keV Si^+ implants with a dose of $2 \times 10^{14} \text{ cm}^{-2}$ and after annealing at 800 °C for 5 min, comparable to our implantation and annealing conditions, showed a dense band of both $\{311\}$ defects and small dislocation loops at a depth of about 200 nm. Upon further annealing, the density of $\{311\}$ defects decreased rapidly and the loop density increased.^{14,15} We suppose that in our case these defects glide to the Si/SiGe interface initiating the formation of misfit dislocations, similar to the relaxation model discussed for the case of H^+ or He^+ implantation¹¹ and are, therefore, not visible in XTEM images in Figs. 2 and 4. In addition, point defect clusters within the SiGe layer may further promote strain relaxation of the layer. They may convert to dislocation loops and form misfit segments at the lower interface. This suggestion is supported by the rather large degree of relaxation of the SiGe layer on SOI (Fig. 4) of 75% since a large fraction (60%) of the implanted Si stops in the underlying SiO_2 and will not contribute to the strain relaxation. These aspects deserve further investigations.

In summary, we have shown that efficient and healthy strain relaxation of pseudomorphic SiGe/Si heterostructures can be achieved by Si^+ ion implantation and annealing. Compared to strain relaxation by He^+ ion implantation,¹⁰ the required Si ion doses of $1\text{--}2 \times 10^{14} \text{ cm}^{-2}$ are two orders of magnitude smaller, therefore allowing high wafer throughput. Threading dislocation densities as low as $3 \times 10^7 \text{ cm}^{-2}$ were achieved. We suggest that strain relaxation is induced by dislocation loops formed in the underlying Si and by defect clusters in the SiGe layer. The process works likewise both with CVD and MBE grown SiGe layers and on SOI substrate wafers as well.

¹J. Welser, J. L. Hoyt, S. Takagi, and J. F. Gibbons, Tech. Dig. - Int. Electron Devices Meet. **1994**, 373 (1994).

²K. Rim *et al.* VLSI Symposium 2002, IEEE 2002 Symposium on VLSI Technology Digest of Technical Papers.

³E. Fitzgerald, Y.-H. Xie, M. Green, D. Brasen, A. Kortan, J. Michel, Y.-J. Mii, and B. Weir, Appl. Phys. Lett. **59**, 811 (1991).

⁴S. Mantl, B. Holländer, R. Liedtke, S. Mesters, H.-J. Herzog, H. Kibbel, and T. Hackbarth, Nucl. Instrum. Methods Phys. Res. B **147**, 29 (1999).

⁵B. Holländer *et al.*, Nucl. Instrum. Methods Phys. Res. B **175-177**, 375 (2001).

⁶S. Christiansen, P. M. Mooney, J. O. Chu, and A. Grill, in *Materials Issues in Novel Si-Based Technology*, edited by W. En, E. C. Jones, J. C. Sturm, S. Tiwari, M. Hinose, and M. Chan, MRS Symposia Proceedings No. 686, Materials Research Society, Pittsburgh, (2002), p. A1.6.

⁷V. S. Avrutin *et al.*, Mater. Sci. Eng., B **89**, 350 (2002).

⁸R. Hull, J. C. Bean, J. M. Bonar, G. S. Higashi, K. T. Short, H. Temkin, and A. E. White, Appl. Phys. Lett. **56**, 2445 (1990).

⁹L. R. Doolittle, Nucl. Instrum. Methods Phys. Res. B **9**, 344 (1985).

¹⁰M. Luysberg *et al.*, J. Appl. Phys. **92**, 4290 (2002).

¹¹H. Trinkaus, B. Holländer, St. Rongen, S. Mantl, H.-J. Herzog, J. Kuchenbecker, and T. Hackbarth, Appl. Phys. Lett. **76**, 3552 (2000).

¹²M. L. David, M. F. Beaufort, and J. F. Barbot, J. Appl. Phys. **93**, 1438 (2003).

¹³J. Li and K. S. Jones, Appl. Phys. Lett. **73**, 3748 (1998).

¹⁴B. Colombeau, N. E. B. Cowern, F. Cristiano, P. Calvo, N. Cherkashin, Y. Lamrani, and A. Clavarie, Appl. Phys. Lett. **83**, 1953 (2003).

¹⁵F. Cristiano *et al.*, Nucl. Instrum. Methods Phys. Res. B **178**, 84 (2001).